# Characterization of two neuronal subclasses through constellation pharmacology

Russell W. Teichert[a,1], Shrinivasan Raghuraman[a], Tosifa Memon[a], Jeffrey L. Cox[a], Tucker Foulkes[a], Jean E. Rivier[b], and Baldomero M. Olivera[a,1]

[a]Department of Biology, University of Utah, Salt Lake City, UT, 84112; and [b]Clayton Foundation Laboratories for Peptide Biology, The Salk Institute, La Jolla, CA 92037

Contributed by Baldomero M. Olivera, June 11, 2012 (sent for review April 18, 2012)

**Different types of neurons diverge in function because they express their own unique set or constellation of signaling molecules, including receptors and ion channels that work in concert. We describe an approach to identify functionally divergent neurons within a large, heterogeneous neuronal population while simultaneously investigating specific isoforms of signaling molecules expressed in each. In this study we characterized two subclasses of menthol-sensitive neurons from cultures of dissociated mouse dorsal-root ganglia. Although these neurons represent a small fraction of the dorsal-root ganglia neuronal population, we were able to identify them and investigate the cell-specific constellations of ion channels and receptors functionally expressed in each subclass, using a panel of selective pharmacological tools. Differences were found in the functional expression of ATP receptors, TRPA1 channels, voltage-gated calcium-, potassium-, and sodium channels, and responses to physiologically relevant cold temperatures. Furthermore, the cell-specific responses to various stimuli could be altered through pharmacological interventions targeted to the cell-specific constellation of ion channels expressed in each menthol-sensitive subclass. In fact, the normal responses to cold temperature could be reversed in the two neuronal subclasses by the coapplication of the appropriate combination of pharmacological agents. This result suggests that the functionally integrated constellation of signaling molecules in a particular type of cell is a more appropriate target for effective pharmacological intervention than a single signaling molecule. This shift from molecular to cellular targets has important implications for basic research and drug discovery. We refer to this paradigm as "constellation pharmacology."**

calcium imaging | conotoxin | sensory neuron | neuronal subtype

Each type of neuron is programmed to have distinctive signal-transduction pathways and electrical properties. At any given anatomical locus in the nervous system, functionally diverse neuronal subtypes are present, which diverge in the specific mix of ion-channel and receptor isoforms expressed. Recently, we demonstrated that different neuronal subclasses exhibit distinct functional phenotypes in response to a panel of pharmacological challenges. We organized such pharmacological challenges into a profiling platform for discriminating between the various neuronal subclasses present in a heterogeneous population of dissociated neurons (1).

In the present study, we demonstrate the feasibility of targeting a minor fraction of dorsal root ganglion (DRG) neurons for comprehensive functional profiling, to the point where the probable physiological role of the neurons characterized can be inferred and a targeted physiological intervention becomes feasible. A key strength of this approach is that it enables the identification and functional characterization of neuronal subclasses that represent only a miniscule fraction of a diverse cell population. A key cellular component in an important physiological circuit often can be present as a very minor component of a tissue with an overwhelming excess of other cell types.

The two subclasses of DRG neurons we analyzed in this study were identified initially by their responsiveness to menthol (1). One subclass included neurons with cell bodies that were, on average, particularly small in diameter (~14 μm, corresponding to a cross-sectional cell area of ~150 $\mu m^2$). Such neurons responded robustly to menthol but not to any of five other challenge compounds (receptor agonists) tested. These neurons also displayed characteristic instability in their cytoplasmic calcium concentration, $[Ca^{2+}]_i$, and did not stain with isolectin B4 (IB4). We previously called these neurons "M+" neurons (1), but here we refer to them as the "M+A−" neuronal subclass [i.e., menthol positive, but ATP and allyl isothiocyanate (AITC or mustard oil) negative]. The second subclass of menthol-responsive DRG neurons had, on average, somewhat larger-diameter cell bodies, although still technically small (~19 μm diameter, corresponding to a cross-sectional cell area of ~270 $\mu m^2$). These neurons responded weakly to menthol and ATP and robustly to AITC and stained with IB4 (1). We refer to these neurons as the "M+A+" neuronal subclass (i.e., menthol, ATP, and AITC positive). In this study, we have broadly assessed the differences in the ion channels and receptors expressed in these two neuronal subclasses. These differences suggested distinct physiological roles for the two neuronal subclasses. We tested our hypotheses by appropriate physiological stimuli, which provided strong corroborative evidence for the proposed divergence in function.

To identify and characterize these menthol-sensitive neurons, we used calcium imaging (Ca-imaging). This technique allowed us to assess the responsiveness of individual cells across the population of cultured DRG neurons to various pharmacological challenge compounds. The individual responses of >100 DRG neurons were monitored simultaneously in each experimental trial. The menthol-responsive neurons encompassed a small fraction of all DRG neurons (1). For this reason, it would have been exceedingly laborious to identify and characterize such neurons by traditional methods for assessing function, such as patch-clamp electrophysiology, particularly given the difficulty in executing lengthy and complex patch-clamp experiments. The work reported here provides proof-of-principle for the feasibility of characterizing a specific neuronal subtype at any particular locus of the nervous system (such as the DRG) through the definition of the cell-specific constellation of ion channels and receptors expressed in that particular neuronal subtype.

## Results

We dissociated lumbar DRG neurons from wild-type C57BL/6 mice for the Ca-imaging experiments described below. In most experiments, the cell bodies of >100 neurons were monitored individually and simultaneously for their responses to various challenges. In general, the cell bodies of neurons have proven to be good surrogates for the proteins that are expressed in axons and nerve endings (2). We used two general types of challenges described previously in ref. 1 and in *SI Materials and Methods*: receptor-agonist challenges (RA challenges) and membrane-potential challenges (MP challenges). Menthol, ATP, and AITC are

Author contributions: R.W.T. and B.M.O. designed research; R.W.T., S.R., T.M., J.L.C., and T.F. performed research; J.E.R. contributed new reagents/analytic tools; R.W.T., S.R., and T.M. analyzed data; and R.W.T. and B.M.O. wrote the paper.

The authors declare no conflict of interest.

[1]To whom correspondence may be addressed. E-mail: russ.teichert@utah.edu or olivera@biology.utah.edu.

This article contains supporting information online at www.pnas.org/lookup/suppl/doi:10.1073/pnas.1209759109/-/DCSupplemental.

RA-challenge compounds that we used to identify neurons that expressed TRPM8 channels (menthol receptor), ATP receptors, and TRPA1 channels (mustard-oil receptor), thus identifying M+A− and M+A+ neurons. Concurrent with these RA challenges, we used MP challenges to identify the isoforms of functionally expressed voltage-gated ion channels. Table 1 provides abbreviations for all compounds cited in figures. Table S1 provides a summary of additional information about these compounds, including their molecular targets and the working concentrations used (except as otherwise indicated in figure legends).

**Menthol-Elicited Increases in $[Ca^{2+}]_i$ Were Amplified by $K_V1$ Blockers in M+A+ Neurons but Not in M+A− Neurons.** Fig. 1 shows selected Ca-imaging traces for M+A+ neurons (Fig. 1*A*) and for M+A− neurons (Fig. 1*B*). The M+A+ neurons in Fig. 1*A* responded weakly to ATP and menthol but responded strongly to AITC, with transient increases in $[Ca^{2+}]_i$. In contrast, the M+A− neurons in Fig. 1*B* responded strongly to menthol but did not respond to either ATP or AITC with an increase in $[Ca^{2+}]_i$. Notably, when the bath solution was exchanged for bath solution containing ATP, there was a dip (i.e., decrease in $[Ca^{2+}]_i$) in the M+A− neurons, which also occurred when the bath solution was merely replaced with identical room-temperature bath solution that did not contain ATP (Fig. 1*B*). This baseline dip was typically followed by a slow increase in $[Ca^{2+}]_i$ and a relatively noisy $[Ca^{2+}]_i$ baseline, also evident in traces of M+A− neurons in subsequent figures.

Fig. 1 demonstrates that menthol-elicited responses from both M+A− and M+A+ neurons were reproducible in the same neuron. After the third application of menthol, α-Dendrotoxin (α-Dtx), a selective blocker of voltage-gated K channels $K_V1.1$, 1.2, and 1.6, was applied to the cells. The application of α-Dtx dramatically amplified the subsequent response to menthol in most of the M+A+ neurons, but the menthol response was not amplified in M+A− neurons (see legend of Fig. 1). The amplification of menthol responses by α-Dtx was readily reversible (Fig. 1*A*). Fig. 1*C* demonstrates that, in addition to α-Dtx, a selective blocker of $K_V1.2$, κM-conopeptide RIIIJ (κM-RIIIJ), also dramatically amplified menthol responses in M+A+ neurons. Notably, the responses to menthol were much weaker in M+A+ neurons than in M+A− neurons before the application of α-Dtx. However, after the application of α-Dtx, menthol responses in some M+A+ neurons were comparable in magnitude to those in M+A− neurons (Fig. 1).

**Potassium-Elicited Increases in $[Ca^{2+}]_i$ Were Inhibited Substantially by L-Type Ca-Channel Blockers in M+A− Neurons but Not in M+A+ Neurons.** Similar to the experimental protocol shown in Fig. 1, we applied menthol, ATP, and AITC to identify M+A− and M+A+ neurons shown in Fig. 2. Following the application of menthol, we depolarized the neurons by applying an elevated concentration of extracellular KCl (high $[K^+]_o$) to activate voltage-gated Ca channels. After the second application of high $[K^+]_o$, we applied Ca-channel blockers to determine their effects

**Table 1. Abbreviations for compounds cited in figures**

| Abbreviation | Compound |
|---|---|
| AITC | Allyl Isothiocyanate (mustard oil) |
| B | Bath replacement at room temperature |
| Dtx | α-Dendrotoxin |
| GVIA | ω-Conopeptide GVIA |
| K | KCl |
| M | Menthol |
| MVIIC | ω-Conopeptide MVIIC |
| Nic | Nicardipine |
| RIIIJ | κM-Conopeptide RIIIJ |
| SNX | SNX-482 |
| T | Tetrodotoxin (TTX) |
| T+Mr | Tetrodotoxin + μO-Conopeptide MrVIB |
| V | Veratridine |

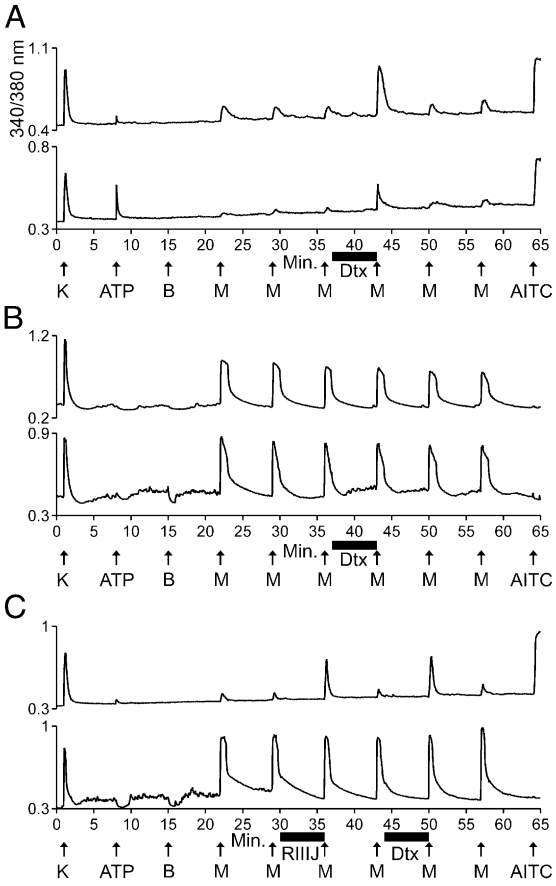


**Fig. 1.** Antagonists of the $K_V1$ family of voltage-gated K channels substantially amplified the response to menthol in M+A+ neurons but not in M+A− neurons. The experimental methods and figure format are described in *Materials and Methods*. Each trace represents the response of a different neuron. In a typical experimental trial, the responses of >100 individual neurons were monitored simultaneously. Selected traces are shown. The aforementioned facts are the same for all subsequent figures. The abbreviations used in all figures are defined in Table 1. (*A*) Two traces from different M+A+ neurons that responded to menthol. Their responses to menthol were amplified reversibly by α-Dtx. After application of α-Dtx, the average menthol-elicited response as a percentage of control peak height was 275 ± 29% for M+A+ neurons ($n$ = 5 trials, 51 cells total). (*B*) Two traces from different M+A− neurons that responded to menthol. Their responses to menthol were not amplified by α-Dtx. After application of α-Dtx, the average menthol-elicited response as a percentage of control peak height was 99 ± 3% for M+A− neurons ($n$ = 5 trials, 16 cells total). (*C*) (*Upper*) Menthol responses in this M+A+ neuron were amplified reversibly by both κM-RIIIJ and α-Dtx. With this experimental protocol, the average menthol-elicited response as a percentage of control peak height was 292 ± 21% after application of κM-RIIIJ and 352 ± 14% after application of α-Dtx for M+A+ neurons ($n$ = 3 trials). (*Lower*) Menthol responses in this M+A− neuron were not amplified significantly by either κM-RIIIJ or α-Dtx. The average menthol-elicited response as a percentage of control peak height was 108 ± 8% after application of κM-RIIIJ and 110 ± 10% after application of α-Dtx for M+A− neurons ($n$ = 3 trials).

on subsequent responses to high $[K^+]_o$. Fig. 2*A* demonstrates that the KCl-elicited $[Ca^{2+}]_i$ signals in M+A− neurons were blocked nearly completely by the L-type ($Ca_V1$) Ca-channel blocker, nicardipine. In contrast, M+A+ neurons were blocked only modestly by nicardipine. From this result, we hypothesized that M+A− neurons functionally express predominantly $Ca_V1$ channels, whereas M+A+ neurons express a complex set of $Ca_V$ channels.

A mixture of $Ca_V2$-family blockers, including ω-conopeptide MVIIC (ω-MVIIC), a selective blocker of N-type ($Ca_V2.2$) and P/Q-type ($Ca_V2.1$) Ca channels, and SNX-482, a selective

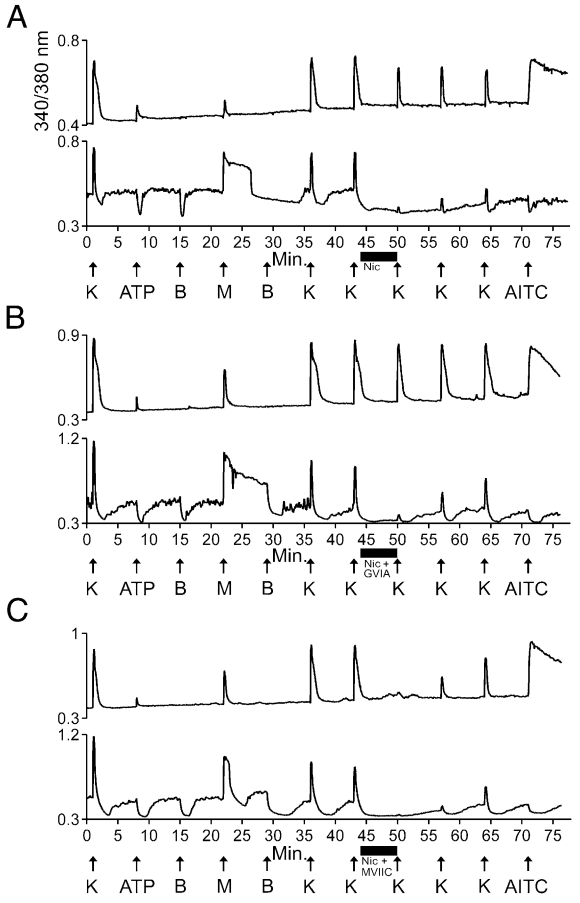


**Fig. 2.** A $Ca_V1$ antagonist blocked the response to high $[K^+]_o$ in M+A− neurons nearly completely, whereas a combination of $Ca_V1$ and $Ca_V2.1$ antagonists was required to achieve a similar degree of block in M+A+ neurons. Menthol was applied at 500 μM working concentration, in contrast to Fig. 1, where 250 μM menthol was used. Application of 500 μM menthol typically produced more robust $[Ca^{2+}]_i$ signals in M+A+ neurons than 250 μM (Fig. 1), but the $[Ca^{2+}]_i$ signals elicited by 500 μM menthol were excessively large in some M+A− neurons. Here, "K" indicates 30 mM KCl. This concentration was used to activate as many voltage-gated Ca channels as possible. Many neurons could not recover from higher concentrations of KCl. (*A*) Nicardipine inhibited the KCl-elicited calcium signals in M+A− neurons nearly completely, but it blocked KCl-elicited calcium signals in M+A+ neurons only modestly: The average KCl-elicited response as a percentage of control peak height was 14 ± 4% for M+A− neurons ($n$ = 4 trials, 11 cells total) and 79 ± 2% for M+A+ neurons ($n$ = 4 trials, 39 cells total). (*B*) GVIA did not augment the block by nicardipine in M+A+ neurons. After application of nicardipine and GVIA. The average KCl-elicited response as a percentage of control peak height was 19 ± 5% for M+A− neurons ($n$ = 4 trials, 9 cells total) and 82 ± 3% for M+A+ neurons ($n$ = 4 trials, 40 cells total). (*C*) The combination of nicardipine and MVIIC substantially inhibited the KCl-elicited calcium signal in both M+A− and M+A+ neurons. After application of the mixture, the average KCl-elicited response as a percentage of control peak height was 9 ± 2% for M+A− neurons ($n$ = 5 trials, 18 cells total) and 24 ± 2% for M+A+ neurons ($n$ = 5 trials, 57 cells total).

blocker of R-type ($Ca_V2.3$) Ca channels, did not block the KCl-elicited calcium signals in M+A− neurons (Fig. S1). In consideration of the nearly complete block shown in Fig. 2*A* with a $Ca_V1$ inhibitor, the lack of block by $Ca_V2$ inhibitors (Fig. S1) further supported the hypothesis that M+A− neurons express predominantly $Ca_V1$ channels. In contrast to its effect in M+A− neurons, the mixture of ω-MVIIC and SNX-482 modestly blocked the KCl-elicited calcium signals in M+A+ neurons (Fig. S1), similar to the partial block of M+A+ neurons by nicardipine shown in Fig. 2*A*. These results led us to test nicardipine in combination with selective $Ca_V2$ inhibitors. Fig. 2*B* demonstrates that the selective $Ca_V2.2$-channel blocker ω-conopeptide GVIA (ω-GVIA) did not increase the block by nicardipine shown in Fig. 2*A*. In contrast, ω-MVIIC in combination with nicardipine blocked nearly all the KCl-elicited calcium signals from M+A+ neurons (Fig. 2*C*). These results suggested that the M+A+ neurons express predominantly a mixture of $Ca_V1$ and $Ca_V2.1$ channels, in contrast to the predominant $Ca_V1$ expression in M+A− neurons.

In support of the hypothesis that M+A− neurons predominantly express $Ca_V1$ channels, Fig. S2 demonstrates that nicardipine substantially blocked the menthol-elicited calcium responses in M+A− neurons, similar to the inhibition of KCl-elicited calcium responses shown in Fig. 2*A*. As expected, the nicardipine block of menthol responses was less, on average, than the block of KCl responses (see legends for Fig. 2 and Fig. S2), because menthol elicits calcium influx through TRPM8 channels, which are not blocked by nicardipine. However, in M+A− neurons the response to menthol apparently is amplified by $Ca_V1$ channels, which are blocked by nicardipine. The nicardipine block exhibited moderately slow reversibility whether in blocking KCl-elicited responses (Fig. 2) or menthol-elicited responses (Fig. S2).

**M+A− Neurons Express Predominantly TTX-Sensitive Voltage-Gated Na Channels, Whereas M+A+ Neurons Express both TTX-Sensitive and TTX-Resistant Voltage-Gated Na Channels.** Veratridine has been used as a chemical activator of voltage-gated Na channels in a variety of cell-based assays. It is reported to have greater potency for tetrodotoxin-sensitive (TTX-S) Na channels than for TTX-resistant (TTX-R) Na channels (3), although we have not found $EC_{50}$ values of veratridine for Na-channel isoforms in the scientific literature. Fig. 3 demonstrates that when we applied 30 μM veratridine to the cultured neurons, it elicited a robust spike in $[Ca^{2+}]_i$ in both M+A− and M+A+ neurons (demarcated by vertical lines in Fig. 3*A*), suggesting the probable expression of TTX-S Na channels. We then tested the effect of applying 1 μM TTX to the neurons before, during, and after the application of 30 μM veratridine. TTX blocked the spike in $[Ca^{2+}]_i$ elicited by veratridine in both M+A− and M+A+ neurons (demarcated by vertical lines in Fig. 3*B*). This result supported the hypothesis that both M+A+ and M+A− neurons functionally express TTX-S Na channels.

Additionally, in the presence of both TTX and veratridine, the KCl-elicited increase in $[Ca^{2+}]_i$ (peak height) was amplified in M+A+ neurons (upper trace in Fig. 3*B* and Table 2) but was partially blocked in M+A− neurons (lower trace in Fig. 3*B* and Table 2). We hypothesized that M+A− neurons expressed only TTX-S Na channels, because of the observation that TTX completely blocked the veratridine-elicited response and also partially blocked the KCl-elicited response following the application of veratridine. Although on average the KCl-elicited responses in M+A− neurons were partially blocked by TTX (Table 2), there were a few uncommon instances in which the KCl-elicited $[Ca^{2+}]_i$ peak exhibited some broadening but no increase in peak height (Fig. S3). Thus, we cannot rule out the possibility that a few of the M+A− cells express low levels of TTX-R Na channels, such as $Na_V1.8$ or $Na_V1.9$, that may be responsible for such peak broadening in the presence of veratridine and TTX. However, the summary data from Table 2 indicate that M+A− neurons express predominantly TTX-S Na channels.

From the amplification observed in the upper trace in Fig. 3*B* (in contrast to the block in the lower trace), we hypothesized that the observed amplification was caused by veratridine activity on TTX-R Na channels, particularly $Na_V1.8$, which is required for action-potential generation in a subset of small-diameter DRG neurons (4). Although veratridine is an effective activator of TTX-S Na channels (Fig. 3 and ref. 3), it is not an effective activator of $Na_V1.8$ (3). However, veratridine is known to bind Na channels in the open state and prevent fast inactivation (3), consistent with the hypothesis. We tested the hypothesis by executing the experimental protocol depicted in Fig. 3*B* with DRG neurons from $Nav1.8^{-/-}$ mice. Example traces from these results are shown in Fig. S4, and the data are summarized in Table 2. The amplification observed in the presence of veratridine and

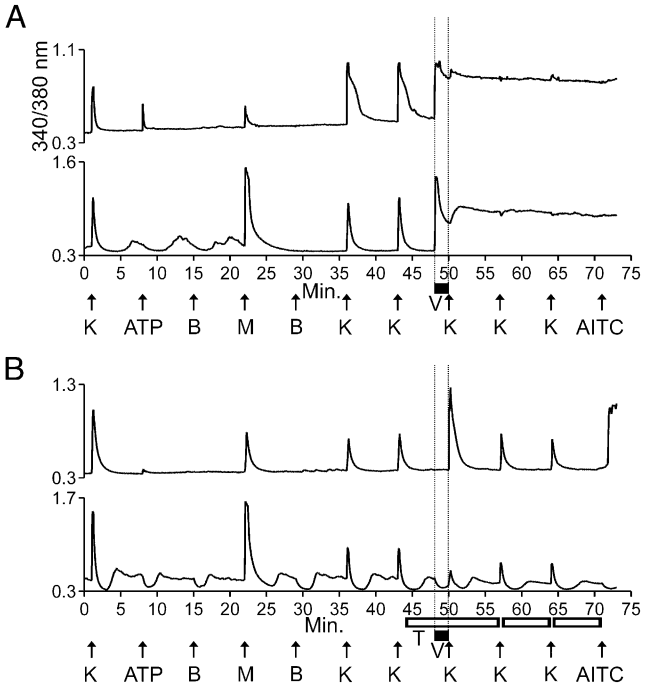


**Fig. 3.** Veratridine-elicited responses were blocked by TTX in both M+A− and M+A+ neurons. However, in the presence of both TTX and veratridine, KCl-elicited responses were amplified in M+A+ neurons but were blocked in M+A− neurons. The vertical dashed lines are for clarity only, indicating when veratridine was present in the well. (*A*) Both M+A− and M+A+ neurons responded immediately to application of veratridine (black bar) with an elevated and sustained increase in $[Ca^{2+}]_i$. Here, "K" indicates 20 mM KCl. (*B*) The immediate responses to veratridine shown between the vertical dashed lines in *A* were blocked by TTX (open horizontal bars) in both M+A− and M+A+ neurons. However, in the presence of both TTX and veratridine, KCl-elicited responses were amplified in M+A+ neurons (*Upper*) but were partially blocked in M+A− neurons (*Lower*). After application of veratridine and TTX, the average KCl-elicited response as a percentage of control peak height was 271 ± 16% for M+A+ cells ($n$ = 6 trials, 56 cells total) and 81 ± 10% for M+A− cells ($n$ = 6 trials, 15 cells total). Here, "K" indicates 25 mM KCl at minute 1 and then 15 mM KCl at subsequent time points (15 mM KCl was used because it made the amplification observed in the upper trace of *B* more evident, while the block observed in the lower trace of B remained clear).

TTX in M+A+ neurons from WT mice (Fig. S4*A*) was not observed in $Na_V1.8^{-/-}$ mice (Fig. S4*B*). In contrast, we observed a partial block of the KCl-elicited peak after application of TTX and veratridine in M+A+ neurons from $Na_V1.8^{-/-}$ mice (Fig. S4*B* and Table 2).

We further tested the hypothesis that M+A+ neurons express $Na_V1.8$ by coapplying TTX and μO-conopeptide MrVIB (μO-MrVIB, a selective blocker of $Na_V1.8$) to WT neurons before and during the application of veratridine. The amplification observed in the presence of veratridine and TTX in M+A+ neurons from WT mice (Fig. S4*A*) was not observed in M+A+ neurons from WT mice when both TTX and μO-MrVIB were coapplied in the presence of veratridine (Fig. S4*C*). On average, we observed a partial block of the first KCl-elicited peak following application of these compounds (Fig. S4*C* and Table 2). Cumulatively, the results summarized in Table 2 supported the hypothesis that M+A+ neurons express both TTX-S and TTX-R Na channels.

**M+A− Neurons Responded to Innocuous Cool Temperatures, Whereas M+A+ Neurons Responded only to Noxious Cold Temperatures.** Both M+A− and M+A+ neurons responded to menthol, implying that their role in vivo is to detect cold temperatures (5). However, their precise physiological roles may differ as a result of the divergent ion-channel constellations expressed in each subclass. We hypothesized that M+A− neurons are low-threshold cold thermosensors that detect changes in cold temperature gradient without producing pain and that M+A+ neurons are high-threshold, noxious cold-sensing nociceptors that transmit signals of cold pain. Part of the rationale for these hypotheses came from studies with cold-sensitive trigeminal-ganglion neurons, in which low-threshold neurons exhibited high expression of TRPM8 and low expression of $K_V1$ channels, whereas high-threshold neurons exhibited low TRPM8 and high $K_V1$, with $K_V1$ acting as an excitability brake (6). Similarly, we demonstrated with DRG neurons that, relative to M+A+ neurons, M+A− neurons responded strongly to menthol (Figs. 1–3), suggesting high expression of TRPM8, but they lacked sensitivity to $K_V1$ blockers (Fig. 1; also see ref. 1 for additional $K_V1$ blockers used in our previous study), suggesting low expression of $K_V1$ channels. In contrast, the M+A+ neurons exhibited weak responses to menthol, suggesting low expression of TRPM8, but such responses were dramatically amplified by $K_V1$ blockers, suggesting high expression of $K_V1$ channels (Fig. 1).

Additionally, M+A− neurons exhibited noisy resting $[Ca^{2+}]_i$ and a dip in the $[Ca^{2+}]_i$ baseline each time the static-bath solution was exchanged, suggesting that these cells might respond to minor changes in bath temperature. Hypothetically, the dip may be caused by transient slight warming each time the solution is exchanged, on a slightly cool background caused by evaporative cooling of the static bath. In contrast to M+A− neurons, M+A+ neurons did not exhibit such fluctuations in $[Ca^{2+}]_i$. Furthermore, the expression of $Na_V1.8$ has been shown to be essential for pain at noxious cold temperatures (7). We demonstrated that M+A+ neurons express $Na_V1.8$, but M+A− neurons do not (Fig. 3, Fig. S4, and Table 2). Cumulatively, these data support the hypotheses that M+A− neurons are low-threshold cold thermosensors and that M+A+ neurons are high-threshold, noxious cold-sensing nociceptors.

We directly tested the hypotheses that M+A− neurons are low-threshold cold thermosensors and that M+A+ neurons are high-threshold cold nociceptors in the following way. Fig. 4 demonstrates that M+A− neurons in culture responded to both 17 °C and 4 °C with elevated $[Ca^{2+}]_i$ (Fig. 4*D*), supporting the hypothesis that these neurons are thermosensors that respond to innocuous cool temperatures (17 °C). In contrast to M+A− neurons, M+A+ neurons responded only to 4 °C and not to 17 °C (Fig. 4*C*), supporting the hypothesis that these neurons are nociceptors that respond only to noxious cold (4 °C). Fig. 4 also shows traces from neurons in the same imaging experiment (same field of view) that did not respond to menthol or cold with elevated $[Ca^{2+}]_i$. Rather, most neurons responded to 4 °C with a slight downward inflection in their calcium signal, suggesting a slight decrease in $[Ca^{2+}]_i$ in response to extreme cold (Fig. 4 *A* and *B*). Presumably such neurons do not sense cold temperatures and serve different physiological roles.

**Cold-Elicited Responses Were Amplified by $K_V1$ Blockers in M+A+ Neurons but Not in M+A− Neurons.** We then tested the hypothesis that the cold responses in M+A+ neurons would be amplifiable by $K_V1$ blockers but that the cold responses in M+A− neurons would not be amplifiable. Similar to the amplification of menthol-elicited calcium signals shown in Fig. 1, α-Dtx amplified the responses to cold in M+A+ neurons, but not in M+A− neurons (Fig. S5). The effects of α-Dtx were readily reversible (Fig. S5). In six different experimental trials, virtually all M+A+ neurons responded only to 4 °C and not to 17 °C, whereas all M+A−

**Table 2. Average peak height as percentage of control ± SEM in the presence of 30 μM Veratridine and 1 μM TTX**

| | M+A+ neurons | M+A− neurons |
|---|---|---|
| WT Mice | 271 ± 16% (56 cells) | 81 ± 10% (15 cells) |
| $Na_V1.8^{-/-}$ mice | 76 ± 12% (58 cells) | 69 ± 9% (10 cells) |
| WT Mice + 1 μM μO-MrVIB | 76 ± 4% (74 cells) | 54 ± 6% (19 cells) |

Each average ± SEM is from ≥ four independent trials.

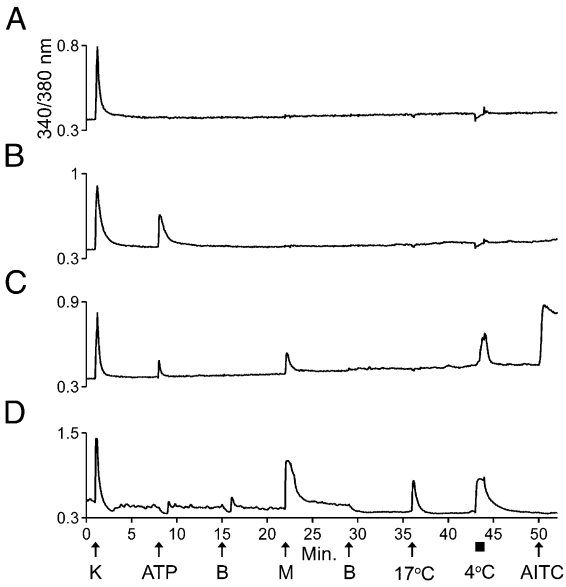


**Fig. 4.** M+A− neurons responded to innocuous cool temperatures and noxious cold temperatures, but M+A+ neurons responded only to noxious cold temperatures. (*A* and *B*) Traces from neurons in the culture that did not respond to menthol or cold temperatures with an increase in $[Ca^{2+}]_i$. (*A*) One neuron responded only to application of KCl. (*B*) The other neuron responded to KCl and ATP. In these two neurons, the slight downward inflection in the baseline observed when 4 °C bath solution was applied to the well suggests a decrease rather than an increase in $[Ca^{2+}]_i$. (*C*) A trace from an M+A+ neuron that responded to noxious cold temperature (4 °C, 1-min application) but not to innocuous cool temperature (17 °C). The response to 4 °C reached its maximum relatively slowly over the time course of the application. (*D*) A trace from an M+A− neuron that responded to cool temperature (17 °C, 15-s application) and noxious cold temperature (4 °C). The M+A− neuron reached a maximum response to 4 °C quickly, and the calcium signal plateaued for the duration of the application.

neurons responded to both 4 °C and 17 °C. In a few cases, however, the M+A+ neurons responded very weakly to 17 °C (Fig. S5).

**Constellation Pharmacology Demonstrated by the Combination of Nicardipine and κM-RIIIJ.** The constellation pharmacology paradigm suggests that we can achieve desired physiological effects in particular cell types by targeting combinations of molecular targets expressed in those particular cell types. We have shown that the response to either cold or menthol in M+A+ neurons was amplified dramatically by $K_V1$ blockers (Fig. 1 and Fig. S5), whereas their KCl-elicited depolarizations were blocked only modestly by nicardipine (Fig. 2). In contrast, the response to either cold or menthol in M+A− neurons was not amplified by $K_V1$ blockers (Fig. 1 and Fig. S5), whereas their KCl- and menthol-elicited calcium signals were blocked substantially by nicardipine (Fig. 2 and Fig. S2). Thus, we hypothesized that by coapplying nicardipine and κM-RIIIJ, we would amplify the response to cold in M+A+ neurons and block the response to cold in M+A− neurons. In fact, we demonstrated these contrasting effects by coapplication of these compounds in Fig. 5.

## Discussion

**Summary of Differences Between M+A− and M+A+ Neurons.** In this study, we characterized two neuronal subclasses among the functionally diverse DRG neurons: One subclass of exceptionally small-diameter neurons (M+A− neurons) responded to menthol, but not to ATP or AITC, whereas a second subclass (M+A+ neurons) responded to all three compounds. In M+A− and M+A+ neurons we evaluated the functional expression of voltage-gated K-, Ca-, and Na-channel isoforms as well as physiologically relevant challenges, i.e., cold temperatures. By every protocol, the two subclasses differed. These differences are summarized in Table 3.

Both M+A− and M+A+ neurons likely function as cold-sensing neurons, as suggested by their menthol responses (5). However, data from this study and others (6, 7) led us to hypothesize that these two neuronal subclasses serve divergent physiological roles in vivo. M+A− neurons responded robustly to innocuous cold temperatures (17 °C), but M+A+ neurons responded only to noxious cold (4 °C). Because 15 °C is considered the approximate separation point between innocuous and noxious cold (5, 8, 9), the data support the hypothesis that the M+A− neurons are thermosensors that respond to innocuous cold-temperature gradients without pain, whereas the M+A+ neurons are thermo-nociceptors that respond to noxious cold temperatures with the sensation of pain. The M+A+ neurons may be nociceptors that detect extreme cold with a sensation of burning pain, consistent with the coexpression of TRPM8 and TRPA1 in the same neuron (6, 10, 11) and the role of $Na_V1.8$ in these neurons (7).

In addition to the differences summarized above, M+A− neurons exhibited a much stronger response to either menthol or cold temperature than do the M+A+ neurons. However, these differences could be altered by targeted pharmacological interventions, thus indicating that the magnitude of the response is not primarily a consequence of differences in the level of TRPM8 expression. Instead, the magnitude of the response is mainly a function of differences in the constellations of ion channels expressed in M+A+ vs. M+A− neurons. In M+A− neurons, the addition of $K_V1$ blockers did not change the response to menthol or noxious cold, whereas in M+A+ cells there was a striking amplification in response. Such amplification may be caused by an increase in input resistance caused by blocking $K_V1$ channels.

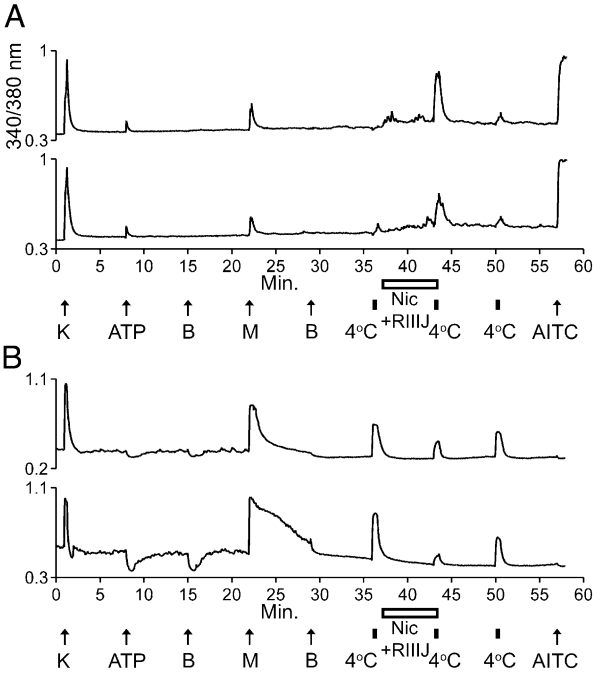


**Fig. 5.** The combination of nicardipine and κM-RIIIJ blocked responses to cold in M+A− neurons but amplified responses to cold in M+A+ neurons. Note that each application of 4 °C bath solution was for 30 s, designated by small black bars. Coapplication of nicardipine and κM-RIIIJ is designated by open horizontal bars. (*A*) Two traces from different M+A+ neurons. Their responses to 4 °C bath solution were amplified by a combination of κM-RIIIJ and nicardipine. After application of κM-RIIIJ and nicardipine, the average cold-elicited response as a percentage of control peak height was 294 ± 52% for M+A+ neurons ($n$ = 5 trials, 81 cells total). (*B*) Two traces from different M+A− neurons. Their responses to the 4 °C bath solution were partially blocked by a combination of κM-RIIIJ and nicardipine. After application of κM-RIIIJ and nicardipine, the average cold-elicited response as a percentage of control peak height was 46 ± 4% for M+A− neurons ($n$ = 5 trials, 19 cells total).

**Table 3. Constellations of M+A+ and M+A− neurons**

| | M+A+ neurons | M+A− neurons |
|---|---|---|
| $K_V$ channels | High $K_V1$ ($K_V1.2$) | Low $K_V1$ |
| $Ca_V$ channels | $Ca_V1$ & 2.1 | $Ca_V1$ |
| $Na_V$ channels | TTX-S & -R ($Na_V1.8$) | TTX-S |
| TRPM8 | Yes | Yes |
| TRPA1 | Yes | No |
| ATP receptors | Yes | No |
| Cold sensitivity | Noxious cold | Innocuous cold |

In other words, opening TRPM8 channels while $K_V1$ channels are blocked may produce a greater voltage change (more depolarization), which consequently opens more voltage-gated Ca channels. Additionally, we have demonstrated that a response to innocuous cold could be elicited in M+A+ neurons by blocking $K_V1$ channels (Fig. S6). Thus, $K_V1$ channels are functionally coupled to TRPM8 activation in M+A+ cells but not in M+A− cells. Conversely, $Ca_V1$ channels are functionally coupled to TRPM8 activation in M+A− cells, as demonstrated by the fact that a $Ca_V1$ blocker substantially inhibited the response to menthol. Thus, the activation of TRPM8 is amplified by activation of $Ca_V1$ channels in M+A− neurons but is attenuated almost immediately by the activation of $K_V1$ channels in M+A+ neurons. This native functional coupling was confirmed when we pharmacologically uncoupled TRPM8 activation from both $Ca_V1$ and $K_V1$activation (by coapplying κM-RIIIJ and nicardipine). The normal responses to cold were completely reversed: The responses from the M+A+ neurons became relatively larger than the responses from the M+A− neurons.

**Potential for Constellation Pharmacology in Basic and Applied Research.** The experiments conducted in this study differ from the standard pharmacological approach for understanding physiology, which conventionally focuses on one molecular target at a time. In contrast, we have broadly examined the constellations of ion channels and receptors expressed in two neuronal subclasses. This examination subsequently enabled us to investigate the functional integration of certain components in each constellation. This research has been facilitated by the ever-increasing availability of ligands that selectively target a single molecular isoform of related proteins (e.g., receptors and ion channels). In principle, this methodology can be applied to any heterogeneous population of neurons.

The functional coupling of TRPM8 and $K_V1$ channels in M+A+ neurons, in contrast to the coupling of TRPM8 and $Ca_V1$ channels in M+A− neurons, illustrated the fact that functionally coupled components may produce divergent physiological responses to the same external input stimuli. This insight is critically important for pharmacological intervention, because perturbing a specific signaling molecule may produce different effects in different cell types, a fact that often is ignored or underappreciated in pharmacology. For example, it has been shown that a mutation in one Na-channel isoform, $Na_V1.7$, produces hyperexcitability in DRG neurons but hypoexcitability in sympathetic ganglion neurons. Whether the mutation results in hypo- or hyperexcitability is determined by the presence or absence of another Na-channel isoform, $Na_V1.8$ (12, 13), which is expressed only in sensory neurons. Thus, the cell-specific constellation is the relevant pharmacological target, rather than an individual signaling molecule.

Shifting the focus from molecular to cellular targets has important implications beyond basic research. In drug discovery, a drug target almost invariably is considered to be a molecule, e.g., a single isoform of a protein. Although this focus on a single molecular target has utility, in some cases it may be overly simplistic, because it fails to take into account the potentially divergent effects of targeting a specific protein in different cell types with different constellations. The focus on a single molecular target also may be unnecessarily limiting, because it offers no flexibility in targeting physiologically relevant cell types to produce a desired physiological end point. In contrast, constellation pharmacology potentially offers substantial flexibility in targeting a cell type of interest. For example, neuronal excitability of the M+A+ subclass could be increased by several different alternative pharmacological strategies using various combinations of ligands, e.g., the application of ATP, menthol, or AITC, block of $K_V1$ channels, activation of $Ca_V1$ and $Ca_V2.1$ channels, or inhibition of $Na_V1.8$ inactivation. Conversely, there would be a similar spectrum of pharmacological strategies to decrease neuronal excitability in M+A+ neurons.

As the cell-specific constellations for a greater diversity of neuronal subtypes become characterized more thoroughly, increasingly sophisticated and more selectively targeted physiological interventions can be used. The ability to discriminate more finely between (and therefore target) individual types of neuronal cells will be facilitated greatly by developing additional ligands specific for individual isoforms of receptors and ion channels, particularly those (such as the K channel family) that can form many different heteromeric combinations.

## Materials and Methods

The experimental methods were approved by the Institutional Animal Care and Use Committee (IACUC) of the University of Utah. Materials and methods have been described in detail previously (1). Additional details are provided in *SI Materials and Methods*. Briefly, all lumbar DRG neurons from C57BL/6 mice >45 d old of both genders were dissociated, pooled, and cultured overnight for Ca-imaging experiments. Mice were WT C57BL/6, except as indicated for a few experiments with $Na_V1.8^{-/-}$ mice (also on the C57BL/6 background). The $Na_V1.8^{-/-}$ mice were kindly provided by Stephen G. Waxman (Yale University, New Haven, CT), with permission from John N. Wood, who produced these mice (14). Cells loaded with Fura-2-AM dye were excited intermittently with 340- and 380-nm light; fluorescence emission was monitored at 510 nm. The ratio of fluorescence intensities (340/380 nm) provided a relative measure of $[Ca^{2+}]_i$, shown as the *y* axis for all traces in all figures (only the upper trace in each figure is labeled). In all figures, the *x*-axis is time in minutes, with labels that apply to all traces in each panel or figure. In the figures, arrows indicate the ∼15-s application of high $[K^+]_o$ or a challenge compound (or cold); horizontal bars indicate times >15 s when challenge compounds were present in the well.

**ACKNOWLEDGMENTS.** This work was supported by Grant GM48677 from the National Institute of General Medical Sciences.

1. Teichert RW, et al. (2012) Functional profiling of neurons through cellular neuropharmacology. *Proc Natl Acad Sci USA* 109:1388–1395.
2. Caterina MJ, Julius D (2001) The vanilloid receptor: A molecular gateway to the pain pathway. *Annu Rev Neurosci* 24:487–517.
3. Farrag KJ, Bhattacharjee A, Docherty RJ (2008) A comparison of the effects of veratridine on tetrodotoxin-sensitive and tetrodotoxin-resistant sodium channels in isolated rat dorsal root ganglion neurons. *Pflugers Arch* 455:929–938.
4. Renganathan M, Cummins TR, Waxman SG (2001) Contribution of Na(v)1.8 sodium channels to action potential electrogenesis in DRG neurons. *J Neurophysiol* 86:629–640.
5. Bautista DM, et al. (2007) The menthol receptor TRPM8 is the principal detector of environmental cold. *Nature* 448:204–208.
6. Madrid R, de la Peña E, Donovan-Rodriguez T, Belmonte C, Viana F (2009) Variable threshold of trigeminal cold-thermosensitive neurons is determined by a balance between TRPM8 and Kv1 potassium channels. *J Neurosci* 29:3120–3131.
7. Zimmermann K, et al. (2007) Sensory neuron sodium channel Nav1.8 is essential for pain at low temperatures. *Nature* 447:855–858.
8. Hensel H, Zotterman Y (1951) The effect of menthol on the thermoreceptors. *Acta Physiol Scand* 24:27–34.
9. Rainville P, Chen CC, Bushnell MC (1999) Psychophysical study of noxious and innocuous cold discrimination in monkey. *Experimental Brain Research* 125(1):28–34.
10. Jordt SE, et al. (2004) Mustard oils and cannabinoids excite sensory nerve fibres through the TRP channel ANKTM1. *Nature* 427:260–265.
11. McKemy DD (2005) How cold is it? TRPM8 and TRPA1 in the molecular logic of cold sensation. *Mol Pain* 1:16.
12. Rush AM, et al. (2006) A single sodium channel mutation produces hyper- or hypoexcitability in different types of neurons. *Proc Natl Acad Sci USA* 103:8245–8250.
13. Waxman SG (2012) Sodium channels, the electrogenisome, and the electrogenistat: Lessons and questions from the clinic. *J Physiol*, 10.1113/jphysiol.2012.228460.
14. Akopian AN, et al. (1999) The tetrodotoxin-resistant sodium channel SNS has a specialized function in pain pathways. *Nat Neurosci* 2:541–548.